



Article

Accumulation of Elements in Biodeposits on the Stone Surface in Urban Environment. Case Studies from Saint Petersburg, Russia

Katerina V. Sazanova (nee Barinova)^{1,2,3,*}, Marina S. Zelenskaya¹ , Vera V. Manurtdinova⁴,
Alina R. Izatulina¹ , Aleksei V. Rusakov¹ , Dmitry Yu. Vlasov^{1,2} and Olga V. Frank-Kamenetskaya¹

¹ Saint Petersburg State University, University Emb., 7/9, 199034 Saint Petersburg, Russia; marsz@yandex.ru (M.S.Z.); alina.izatulina@mail.ru (A.R.I.); alex.v.rusakov@gmail.com (A.V.R.); dmitry.vlasov@mail.ru (D.Y.V.); o.frank-kamenetskaia@spbu.ru (O.V.F.-K.)

² Komarov Botanical Research Institute of Russian Academy of Science, Professor Popov Street, 2, 197376 Saint Petersburg, Russia

³ The Archive of the Russian Academy of Sciences, University Emb., 1, 199034 Saint Petersburg, Russia

⁴ State Museum of Urban Sculpture, Nevsky Prospect 179, 191167 Saint Petersburg, Russia; ver4ik21@mail.ru

* Correspondence: Ksazanova@binran.ru; Tel.: +7-965-078-93-12

Abstract: The pattern of elements accumulation in biodeposits formed by living organisms and extracellular products of their metabolism (biofouling, primary soils) on different bedrocks (of the monuments of Historical necropoleis in Saint Petersburg) were studied by a complex of biological and mineralogical methods (optical microscopy, SEM, EDX, XRD, ICP MS, XRFs). The content of 46 elements in biodeposits with various communities of microorganisms is determined. The model recreating the picture of the input and selective accumulation of elements in biodeposits on the stone surface in outdoor conditions is assumed. It is shown that the main contribution to the elemental composition of biodeposits is made by the environment and the composition of the microbial community. The contribution of leaching under the action of microbial metabolites of mineral grains, entering biodeposits from the environment, is significantly greater than that of the underlying rock.

Keywords: biodeposits; microbial biomineralization; mosses; fungi; algae; lichens; rocks; environment



Citation: Sazanova (nee Barinova), K.V.; Zelenskaya, M.S.; Manurtdinova, V.V.; Izatulina, A.R.; Rusakov, A.V.; Vlasov, D.Y.; Frank-Kamenetskaya, O.V. Accumulation of Elements in Biodeposits on the Stone Surface in Urban Environment. Case Studies from Saint Petersburg, Russia. *Microorganisms* **2021**, *9*, 36. <https://dx.doi.org/10.3390/microorganisms9010036>

Received: 4 December 2020

Accepted: 21 December 2020

Published: 24 December 2020

Publisher's Note: MDPI stays neutral with regard to jurisdictional claims in published maps and institutional affiliations.



Copyright: © 2020 by the authors. Licensee MDPI, Basel, Switzerland. This article is an open access article distributed under the terms and conditions of the Creative Commons Attribution (CC BY) license (<https://creativecommons.org/licenses/by/4.0/>).

1. Introduction

Natural stone located in the urban environment undergoes intensive biological colonization [1–4]. The lithobiotic microbial community (fungi, algae, bacteria, mosses, and lichens) inhabiting the stone surface interacts with the underlying rock, which leads to additional weathering of stone and organomineral biodeposits (biofouling, young soils) formation on the stone surface, containing organic substances, products of bedrock weathering, as well as various elements getting from the environment (air, soil etc) in addition to the organisms themselves [5]. We use the term biodeposits, meaning the complex and different nature of the accumulation of biological objects and products of their vital activity on a solid substrate [6]. Biodeposits include biofouling (microorganisms, lichens, mosses), as well as primary soils under mosses together with organic and mineral components from the outdoor environment and the underlying substrate.

Under the influence of aggressive metabolic products, extracellularly secreted by microorganisms, primarily organic acids, bedrocks dissolve, which contributes to the leaching of microelements from rock, their accumulation in biodeposits, and an increase in their mobility and bioavailability. Probably, biodeposits can also accumulate elements, including heavy metals, leached by the products of microbial metabolism from the grains of minerals that have entered them from the environment. If there is oxalic acid (secreted by many fungi, lichens, as well as a number of bacteria) among the metabolic products,

elements accumulating in biofilms can react with it, which leads to the formation of oxalic acid salts, primarily calcium oxalates [3,7–18]. Unlike the organic component of biodeposits heavy metals are not biodegradable and can transfer through the food chain and are susceptible to bioaccumulation [19].

It is known that the accumulation of elements by the microbial community can be carried out extracellularly and intracellularly [8–10,19–21]. Numerous data indicate an important role of the sorption mechanism on the surface of cell walls when the accumulation of cations by bacteria, microalgae, microfungi, lichens, and mosses [22–30]. The cell wall can take part in the sorption of ions even in the absence of physiological activity (as dead biomass) [19]. The extracellular accumulation of cations can be accompanied by ion exchange [20], leading to the formation of complexes in which the cations are coordinated by the organic functional groups of the cell walls [21]. In addition, extracellular accumulation of elements in biodeposits formed by lichens and fungi can occur through the binding of cations with small organic molecules, primarily organic acids. Organic acid production activity (oxalic, citric, malic, gluconic, fumaric, succinic and some others) is a characteristic of many species of fungi and some lichens [31–33].

Intracellular accumulation of elements can occur through the absorption of metals as a result of the work of transport systems. Once in the cell, the metal can be immobilized inside the vacuoles in the cytoplasm. The mechanisms of metal immobilization can involve organic acids or specific proteins (metallothioneins and phytochelatin capable to bind metals through SH-groups) [9,10,19,34].

According to [35], higher concentrations Al, Cr, Fe, Mn, Ni, Ti are recorded in mosses, and Hg, Cd, Pb, Cu, V, Zn in lichens. Apparently, the concentrations of most elements in mosses are more dependent on the chemical composition of rainwater fallen over a short period, rather than over the whole season, as in the case of lichens [36].

The known features of the accumulation of metals and other elements by organisms of various taxonomic and ecological groups are actively used in biotechnology. Mosses and lichens are used for bioindication [37–40]. Fungi, due to their ability to hyperaccumulate metals in concentrations exceeding those in the environment, are more often used for bioremediation than other organisms [19]. In addition, fungi have a high degree of resistance to the action of heavy metals, which allows them to survive in an environment with a high concentration of metals and utilize the physiologically active mechanisms for their accumulation [22–24].

Thus, the mechanisms of metal accumulation by organisms of various taxonomic and ecological groups are described in detail in the literature and are being actively studied. However, in natural habitats, biodeposits are usually formed by communities of organisms. There is practically no data on the bioaccumulation of elements in biodeposits at the community level, which does not allow for a complete understanding of the patterns of accumulation of inorganic elements on the surface of different rocks and of the geochemistry of the biodeposits present on them.

In this work we are trying to move forward in this direction and identify a pattern of accumulation of elements in biodeposits on the stone surface in urban environment (case of Saint Petersburg). In particular, we planned to: (a) determine the elemental composition of biodeposits with various species composition of microorganisms on different bedrocks; (b) carry out a comparative analysis of the influence of the bedrock, the environment and the species composition of microorganisms on biodeposit elemental composition; (c) restore (at a model level) the picture of the input and selective accumulation of elements in biodeposits in outdoor environment.

2. Materials and Methods

2.1. Sampling

Biodeposits were collected from the surface of stone monuments of the Historical necropoleis located in the central part of Saint Petersburg. Here, in a small area, there are monuments made of various types of decorative stone, which are practically in the

same outdoor environment and undergo biological colonization. The following types of biodeposits containing various communities of living organisms from the surface of different rocks were collected (Table 1, Figure 1): I—biofilms with a predominance of microscopic fungi and algae; II—biofilms with a predominance of lichens; III—vegetative biomass of the moss; IV—primary soil under the moss cover. Although the composition of lichens on the surface of stone monuments includes both crustose and foliose forms we took only samples of foliose lichens, since they have a large biomass, are relatively easy to take from the surface, and also create special conditions for the development of accompanying microorganisms, such as, for example, fungi.

The structural and textural features as well as the mineral composition of the rocks of the monuments of the necropoleis were previously investigated by us, and on this basis, assumptions about their origin were made [41]. Using this data we selected underlying rocks (granites, marbles, limestones) differing in mineral and elemental composition, as well as in their petrographic characteristics (primarily homogeneity and porosity) (Tables 1 and 2), i.e., properties significantly influencing the intensity of weathering and the rate of diffusion of elements from the bedrock into the biodeposits on its surface. When selecting biodeposits we used their morphological properties, studied by us earlier [42].

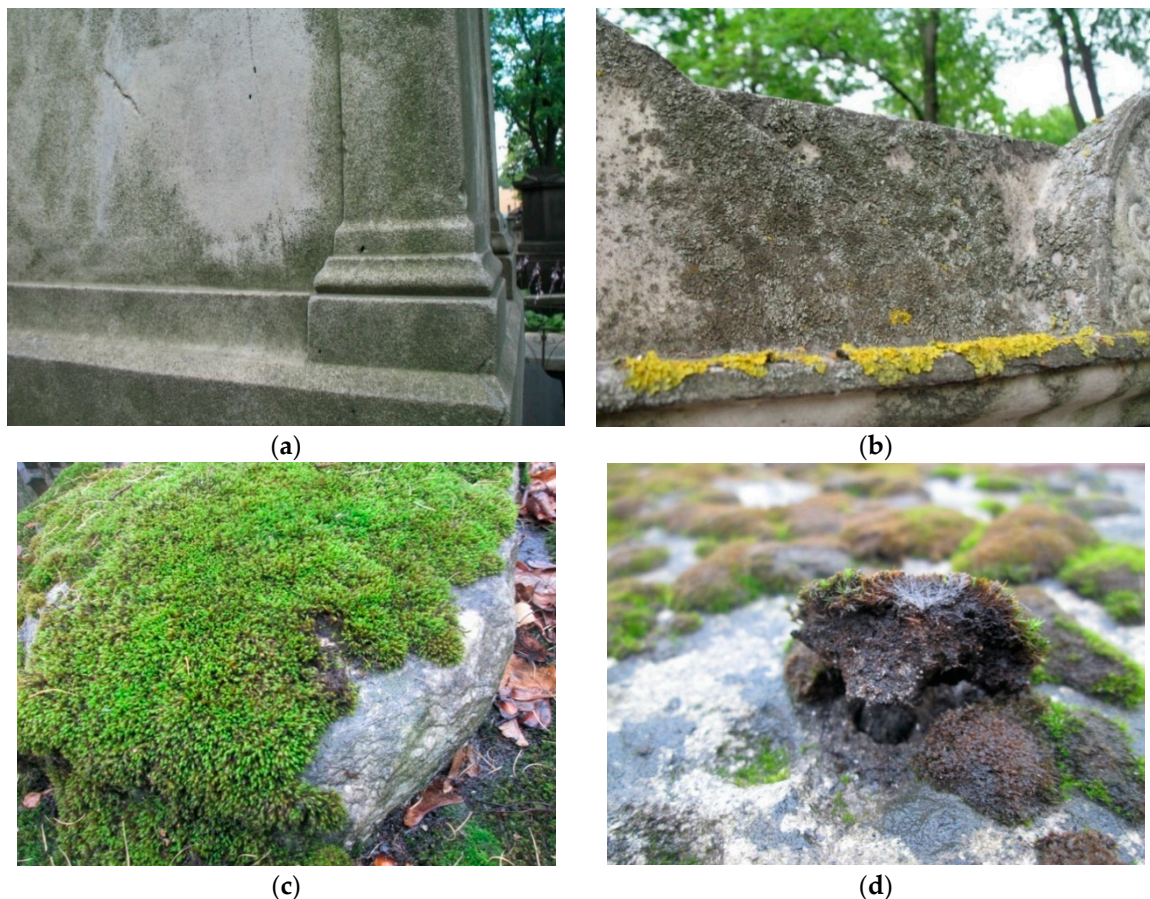


Figure 1. The main types of biodeposits on the surface of stone monuments of the historical necropoleis: (a)—biofilm with a predominance of microscopic fungi and algae; (b)—biofilm with a predominance of lichens; (c)—vegetative biomass of a moss; (d)—primary soil under the moss cover.

Table 1. List of the biodeposits samples collected from Saint Petersburg necropoleis monuments.

Sample	Monument	Underlying rock	
I type. Biodeposits with a predominance of microscopic fungi and algae			
A 1	A. E. Martynov, NMA ¹	Grey homogeneous granite	
A 2	M. P. Zotova, N-18 ²		
II type. Biodeposits with a predominance of lichens			
L 1	E. H. Minich, N-18	Grey porous travertine	
L 2	B. M. Kustodiev, NMA	Wood	
III and IV types. Vegetative biomass of the moss and primary soil under the moss cover.			
M1v ³ , M1s ⁴	M. S. Zotova, N-18	White homogeneous marble	
M2v, M2s	E. A. Rummel, N-18	Grey-white banded heterogeneous marble	
M3v, M3s	T. D. Von-Fewson, N-18		
M4v, M4s	G. I. Ogarev, N-18	Stratified limestone	
M5v, M5s	I. A. Myasnikov, N-18		
M6v, M6s	T. A. Vetoshnikova, N-18		
M7v, M7s	V. S. Bespalov, N-18		
M8v, M8s	A. O. Miklashevich, N-18		
M9v, M9s	Lions, NMA		Grey porous travertine
M10v, M10s	E. D. Chaplina, N-18		Pink ovoid granite
M11v, M11s	A. N. Avdulin, N-18		
M12v, M12s	P. V. Skvortsov, N-18		
M13v, M13s	Monument of Unknown, N-18		
M14v, M14s	B. M. Kustodiev, NMA	Wood	

Notes: ¹ NMA—Necropoleis of Master of Art; ² N-18—Necropoleis of the 18th century; ³ v—vegetative biomass of the moss; ⁴ s—primary soil under the moss cover.

Table 2. Mineral and petrographic characteristics of underlying rocks [41].

No.	Description	Mineral Composition	Assumed Deposit (Geological Age)	Samples of Biodeposits (Table 1)
Marbles				
1	White homogeneous, fine to medium grained marble (statuary marble)	Calcite, quartz	Carrara, Italy (Cretaceous)	M1v, M1s
2	Grey-white banded, heterogeneous, heterogranular carbonate-silicate rock (Ruskeala marble)	Calcite, dolomite, amphiboles (tremolite, hornblende), talc, Fe, Mg—micas, pyroxenes (diopside etc), quartz, apatite	Ruskeala, Karelia, Sortovalva region, Russia (Early Proterozoic)	M2v, M2s

Table 2. Cont.

No.	Description	Mineral Composition	Assumed Deposit (Geological Age)	Samples of Biodeposits (Table 1)
Limestones				
3	Grey, porous travertine (Pudostskii stone)	Calcite, dolomite, quartz	Pudostskoe, Leningrad region, Russia (Quaternary)	L1, M9v, M9s
4	Grey-yellow, stratified Limestone (Putilovskaya plita)	Dolomite, calcite, quartz, glauconite	Putilovskoe, Leningrad region, Russia (Ordovician)	M3v, M3s, M3v, M3s, M4v, M4s, M5v, M5s, M6v, M6s, M7v, M7s, M8v, M8s
Granites				
5	Gray, fairly homogeneous fine- and medium-grained rock (Serdobol granite)	Feldspars (microcline, acidic plagioclase), quartz, mica (biotite), pyroxenes and amphiboles	Karelia Sortavala region, Russia (Early proterozoic)	A1, A2
6	Pink coarse-grained porphyritic ovoid granite (Rapakivi granite)		Leningrad region, Karelia, Russia and Finland (Proterozoic)	M10v, M10s, M11v, M11s, M12v, M12s, M13v, M13s

In order to reliably reveal the influence of the underlying stone substrate on the elemental composition of biodeposits, we also took two biodeposit samples from an eroded surface of a wooden monument for contrast (one with a predominance of lichens and the other with mosses). In addition, in order to compare the elemental composition of dust with the elemental composition of the rock on which it was formed and the compositions of biodeposits on the same rock, we took a dust sample from the surface of a homogeneous white marble.

The collected material was studied using a complex of biological and mineralogical methods.

2.2. Study of Biodiversity

All samples of biodeposits were characterized by their appearance and dominant species of organisms. The identification of microscopic fungi was carried out by isolating them into a pure culture. For primary isolation, maintenance in culture and identification of micromycetes, Czapek-Dox (HiMedia) culture medium was used. Small fragments of biodeposits were placed on the surface of the nutrient medium in Petri dishes. In addition, washings from the substrate surface were used for inoculation. The resulting cultures were incubated in a thermostat for 2–4 weeks at a temperature of 25 °C until sporulation appearance, after which microscopy and identification by morphological characteristics were carried out in accordance with guidebooks and monographs [43–46]. The species were verified in accordance with the modern nomenclature using the Index Fungorum electronic database [47].

The identification of algae was carried out by morphological characteristics. For this purpose, we performed direct microscopy of samples (by means of Leica DM1000 microscope) after settling in distilled water for a week. To determine the species composition, identifiers and monographs [48] as well as the electronic database AlgaeBase [49] were used.

Identification of lichens was carried out according to the generally accepted method using identifiers [50–52], by means of the Leitz Laborlux S microscope, and stereomicroscope MBS-10. The nomenclature of lichen species has been brought in line with the list of lichens in Scandinavia [50].

Identification of bryophytes was carried out according to morphological characteristics using identifiers [53,54], by means of the Micromed-2 microscope and stereomicroscope MBS-10. The nomenclature of bryophytes has been brought in line with the list of bryophytes in Europe, Macaronesia and Cyprus [55].

2.3. Study of the Mineral Component of Biodeposits

The study of the phase composition of mineral grains in biodeposits was carried out via X-ray powder diffraction by means of Bruker “D2 Phaser” powder X-Ray diffractometer operated with CoK α radiation. X-ray diffraction patterns were collected at room temperature in the range of $2\theta = 5\text{--}70^\circ$ with a step of $0.02^\circ 2\theta$ and a counting time of half second per data point. A sample holder from a single crystal silica slice was used to eliminate the background noise. Phase identification was carried out using the ICDD PDF-2 database (release 2016).

To determine the phase composition of secondary silicate minerals with a high degree of dispersion, which are part of primary soils (type IV of biodeposits), we used oriented preparations obtained by successive precipitation of heavy and light mineral fractions [56].

The distribution and qualitative elemental composition of mineral grains in biodeposits were determined via scanning electron microscopy (SEM) and energy-dispersive X-ray spectroscopy (EDX) methods, respectively. Measurements were performed by means of the Desktop Scanning Electron Microscope TM3000 (Hitachi), which was equipped with OXFORD energy dispersive microanalysis attachment and secondary electron (Everhart-Thornley, UK) detector based on the highly sensitive YAG crystal with the resolution of 0.1Z of the atomic number. The specimens were coated with carbon (~15 nm). Magnification range varied from 100x to 1000x. The EDX spectra were analyzed by means of the EDAX Genesis software package (semiquantitative analysis was performed by standard-less method that is generally reliable for elements with $Z > 10$).

2.4. Quantitative Study of the Elemental Composition of Biodeposits

The main method used for the quantitative determination of the elemental composition of collected bioformations was inductively coupled plasma mass spectrometry (ICP MS). This method was used to determine the content of 37 elements (Na, Mg, Al, K, Ti, Mn, Be, V, Cr, Co, Ni, Cu, Zn, Ga, Rb, Sr, Y, Zr, Nb, Mo, Ag, Sn, Sb, Cs, Ba, La, Ce, Pr, Nd, Sm, Eu, Gd, Tb, Dy, Ho, Er, Tm, Yb, Lu, Hf, W, Th, U) in all biodeposits. The solutions were prepared via two different methods of decomposition: complete acid breakdown and fusion with lithium metaborate [57]. The solution analysis was carried by means of ELAN-DRC-e and Agilent 7700x spectrometers using a computer data processing program which automatically accounts for both isotopic and molecular overlays on mass-spectral analytical lines of the determined elements (analyst G.A. Oleinikova).

The content of Ca, Si and Fe in biodeposits of III and IV types (in mosses and primary soils) was determined by X-ray fluorescence method by means of a vacuum X-ray fluorescence crystal-diffraction scanning spectrometer “SPECTROSCAN MAK-S-GV” (Russia). The samples were preliminarily dried in a drying oven at a temperature of 70°C , crushed, ground to the size of a powder, weighed 2g each, and was pressed into tablets using a hydraulic press.

The determination of Ca, Si, and Fe in biodeposits of types I and II (with a predominance of microscopic fungi + algae and lichens, respectively) due to insufficient amount of material was performed via electron probe microanalysis by means of the scanning electron microscope Camscan-4 equipped with X-ray energy microanalyzer AN-10000 (UK) at a 30 kV acceleration voltage and 2 μm electron beam diameter (analyst Yu. L. Kretser). SEM Calibration Specimens (registered standard number 1413) from Microanalysis consultants Ltd. were used as standards. In order to obtain data on the average composition of the sample, the analysis was carried out in the scanning mode at a magnification of x200. Data processing was performed by means of the ZAF-4/FLS program.

2.5. Statistical Analysis

Statistical analysis was performed via the student's t-test and principal component analysis (PCA) using Microsoft Excel, MetaboAnalyst and Origin Pro software.

3. Results

3.1. Microorganism Species Composition of Studied Biodeposits

Microscopic fungi were present in all types of biodeposits, but in the first type, microfungi, together with algae, formed the basis of the community, while in other types of biodeposits they were represented by individual colonies as mycological analysis showed. The species composition of fungi included: *Alternaria alternata* (Fr.) Keissl., *Alternaria chartarum* Preuss, *Arthrinium phaeospermum* (Corda) M.B. Ellis, *Aureobasidium pullulans* (de Bary and Löwenthal) G. Arnaud, *Botrytis cinerea* Pers., *Cladosporium cladosporioides* (Fresen.) G.A. de Vries, *Cladosporium herbarum* (Pers.) Link, *Cladosporium sphaerospermum* Penz., *Coniosporium* sp., *Didymella glomerata* (Corda) Qian Chen and L. Cai, *Epicoccum nigrum* Link, *Exophiala exophialae* (de Hoog) de Hoog, *Fusarium oxysporum* Schltdl., *Mucor hiemalis* Wehmer, *Paecilomyces divaricatus* (Thom) Samson, Houbraken and Frisvad, *Penicillium brevicompactum* Dierckx, *Penicillium herquei* Bainier and Sartory, *Phaeosclera* sp., *Phialophora asteris* (Dowson) Burge and I. Isaac, *Phoma herbarum* Westend., *Scytalidium lignicola* Pesante, *Talaromyces purpureogenus* Samson, N. Yilmaz, Houbraken, Spierenb., Seifert, Peterson, Varga and Frisvad, *Trichoderma viride* Pers., *Trichocladium griseum* (Traaen) X. Wei Wang and Houbraken.

Most often, dark-colored microscopic fungi *A. alternata*, *Aureobasidium pullulans*, *C. cladosporioides*, which dominated in type I together with algae, was constantly observed in all other types of biodeposits. Algae in type I were represented by species of *Chlorophyta*, mainly genera *Trentepohlia*, *Trebuxia*, and *Desmococcus*. In addition, diatoms were quite commonly found on SEM images.

Lichens dominating in type II biodeposits were represented by the species: *Physcia tenella* (Scop.) DC., *Physconia distorta* (With.) J.R. Laundon, *Candelariella aurella* (Hoffm.) Zahlbr., *Myriolecis crenulata* (Hook.) Śliwa et al., *Myriolecis invadens* (H. Magn.) Śliwa et al., *Xanthoria parietina* (L.) Th. Fr., *Phaeophyscia orbicularis* (Neck.) Moberg, *Verrucaria muralis* Ach.

The species composition of mosses in type III biodeposits included *Brachythecium salebrosum* (Hoffm. ex F. Weber and D. Mohr) Schimp., *Ptychostomum pseudotriquetrum* (Hedw.) J.R. Spence and H.P. Ramsay ex Holyoak and N. Pedersen, *Bryoerythrophyllum recurvirostrum* (Hedw.) P.C. Chen, *Ceratodon purpureus* (Hedw.) Brid., *Schistidium apocarpum* (Hedw.) Bruch and Schimp., *Marchantia polymorpha* L. Common for carbonate and silicate rocks were the species: *S. apocarpum*, *B. salebrosum*, *P. pseudotriquetrum*. *B. recurvirostrum* was found only on Pudozh stone and granite, while *C. purpureus* was found only on marble and wood.

3.2. Phase Composition of Mineral Component of Studied Biodeposits

The results of the study showed that in biodeposits of types I, II, and III, we can find almost all minerals of rocks from which the monuments of the necropolies are made [41]. The most common minerals are typical for granites and other silicate rocks: quartz, feldspars (acidic plagioclase, microcline), pyroxenes, amphiboles, biotite, etc, rocks from which most of the stone monuments of the necropolies were made. The mineral composition of grains varies very little from site to site and does not depend on the underlying rock. This is clearly seen in the example of a biofilm with a predominance of microscopic fungi on the surface of a homogeneous fine-grained calcite marble, in which grains of numerous silicate minerals are present (Figures 2–4).

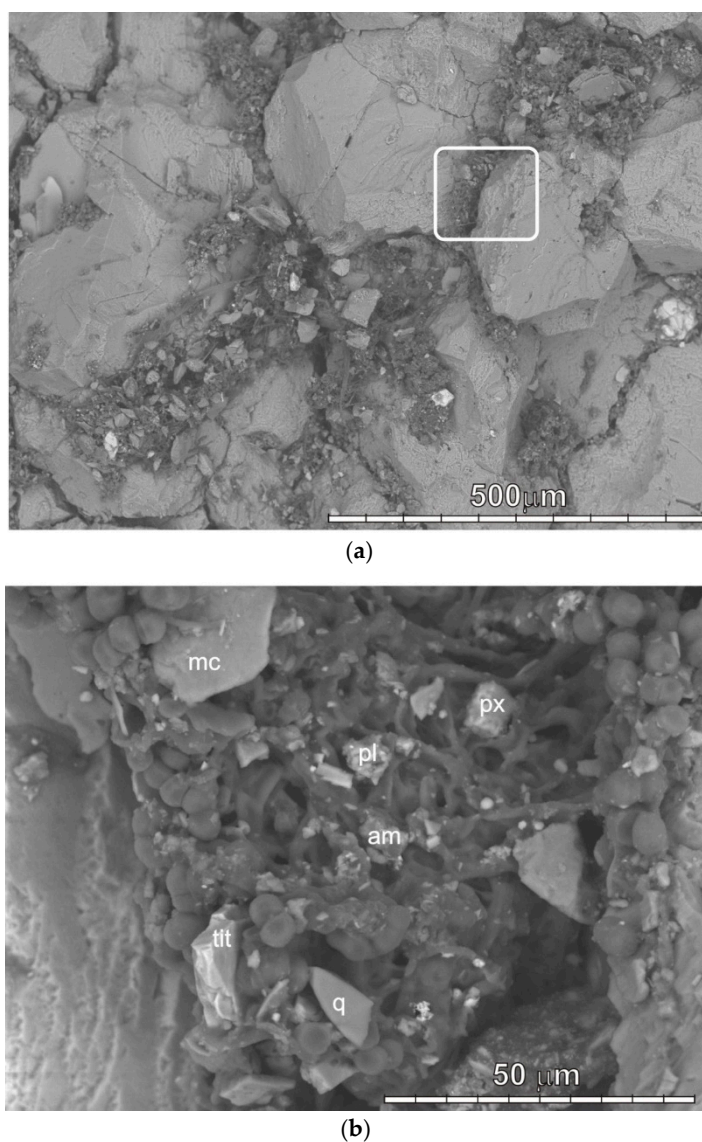


Figure 2. SEM-image of a biofilm with a predominance of microscopic fungi on the surface of a homogeneous calcite marble: (a)—microcolonies of fungi around calcite grains (the white frame shows the area shown in figure b); (b)—grains of various silicate minerals among fungal hyphae and rounded cells (in the region shown in Figure 2a): quartz (q), plagioclase (pl), mica (mc), pyroxene (px), Fe—titanite (tit), Pb—amphibole (am).

In all the samples of primary soils, in addition to minerals found in biofouling there also are secondary layered silicates present in different proportions: mica (biotite, polytype 1M), magnesian chlorite, and disordered mixed-layer silicate of the mica-montmorellonite type.

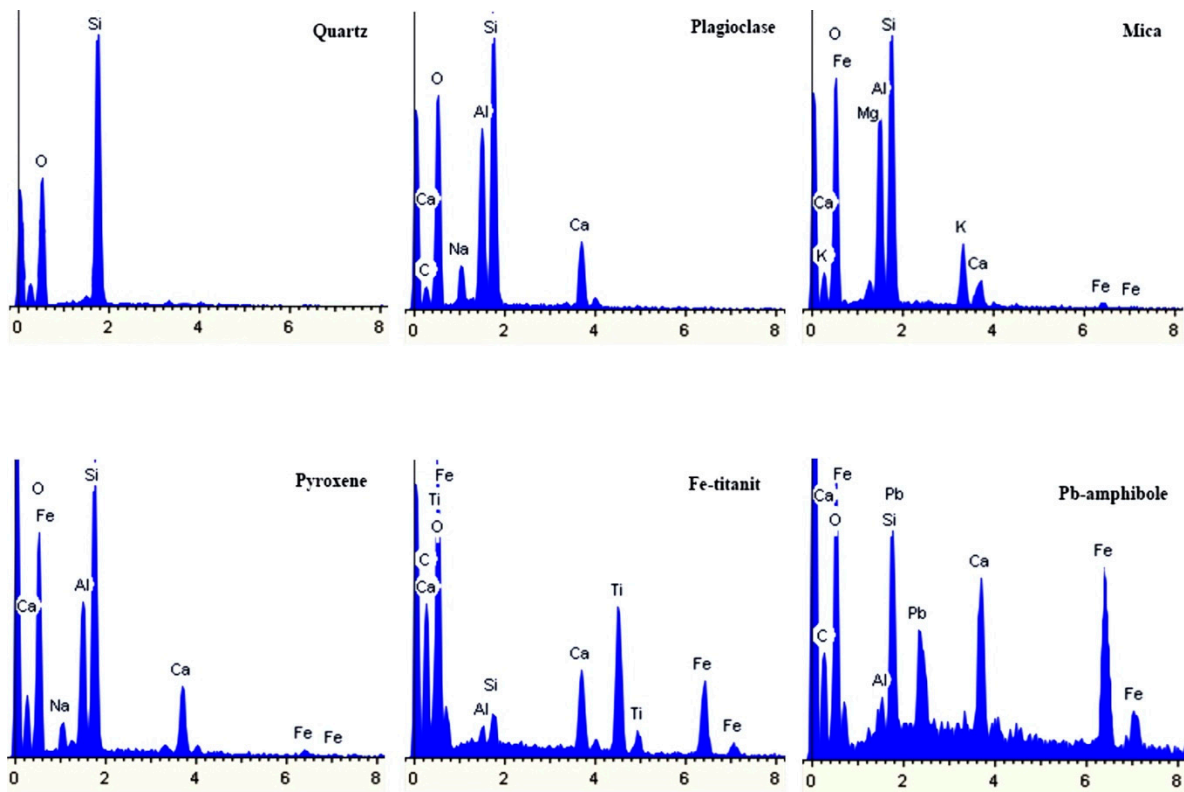


Figure 3. Examples of EDX-spectra of silicate minerals grains in a biofilm with a predominance of microscopic fungi on the surface of a homogeneous calcite marble.

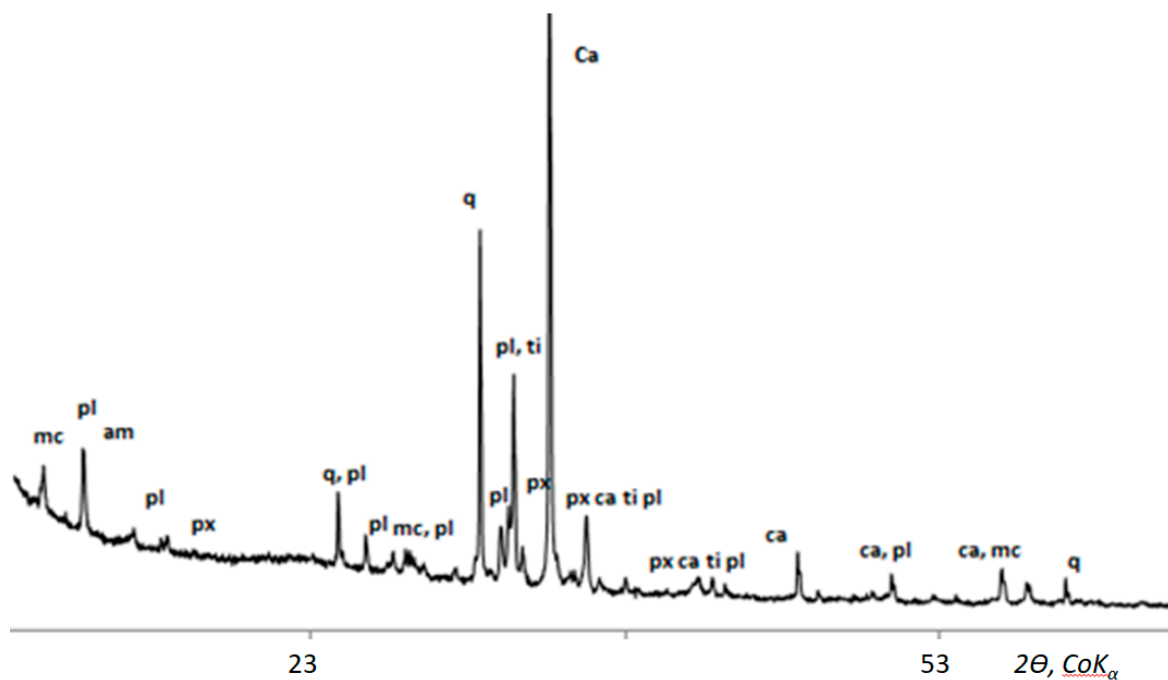


Figure 4. X-ray diagram of silicate minerals grains in biofilm with a predominance of microscopic fungi on the surface of a homogeneous calcite marble: quartz (q), calcite (Ca), plagioclase (pl), mica (mc), pyroxene (px), titanite (ti), amphibole (am).

3.3. Elemental Composition of Biodeposits (Quantitative Data)

46 elements were determined in the studied biodeposits, they can be divided into 2 groups—the main impurity elements, the content of which is not less than 0.2 wt% (in oxide form not less than 0.1 wt%, Figure 5, Table 3) and trace elements, the content of which is less than 0.2 wt% (Figure 6, Table 4).

Type of biodeposits	Underlying rock	№	Element, wt%								
			Na ₂ O	MgO	Al ₂ O ₃	SiO ₂	K ₂ O	CaO	TiO ₂	MnO	FeO
I	Gray granite	A 1	1.2	17.5	8.1	11.1	2.8	1.0	0.7	0.1	1.9
		A 2	2.9	3.0	13.8	13.5	12.3	1.3	1.3	0.2	2.7
II	Grey porous travertine	L 1	3.5	4.0	16.1	5.1	11.1	2.9	1.7	0.2	0.8
	Wood	L 2	2.7	4.1	17.1	17.1	5.0	3.1	2.1	0.2	2.2
III	White marble	M1v	1.6	3.7	9.9	36.1	3.5	4.3	0.8	0.1	8.2
	Ruskeala marble	M2v	1.8	3.7	11.4	42.9	2.6	6.2	1.1	0.1	8.5
	Putilov plate	M3v	1.9	3.4	12.5	22.0	4.7	4.5	0.9	0.1	8.5
		M4v	1.8	3.5	10.0	38.5	3.0	5.5	0.9	0.2	9.1
		M5v	1.9	5.1	12.7	35.1	5.7	6.5	1.0	0.2	6.9
		M6v	1.9	3.8	13.0	23.2	4.6	3.6	0.9	0.2	7.0
		M7v	1.7	4.1	11.2	39.6	4.0	4.3	0.9	0.2	9.6
		M8v	1.7	4.5	11.6	15.0	3.8	2.6	0.9	0.2	9.6
	Grey, porous travertine	M9v	1.3	3.2	8.3	43.9	3.4	5.6	0.7	0.1	9.9
	Pink ovoid granite	M10v	1.6	3.3	10.5	29.8	3.2	4.3	0.8	0.1	7.2
		M11v	1.6	3.6	10.4	63.4	5.6	5.4	0.7	0.1	7.3
		M12v	1.6	3.5	11.7	10.7	4.0	3.5	0.8	0.2	9.3
		M13v	2.0	4.6	12.4	10.2	2.5	2.4	1.1	0.1	12.8
	Wood	M14v	1.7	3.5	11.2	1.9	3.1	1.7	0.9	0.1	7.6
IV	White marble	M1s	1.6	2.0	9.1	50.7	2.3	5.2	0.6	0.1	5.2
	Ruskeala marble	M2s	1.8	2.9	9.9	48.4	1.9	5.4	0.8	0.1	5.4
	Putilov plate	M3s	1.2	2.0	7.7	44.3	2.0	5.9	0.5	0.1	5.9
		M4s	1.6	2.5	9.9	40.8	2.0	5.9	0.8	0.1	3.0
		M5s	2.0	2.4	10.6	48.6	2.0	4.6	1.1	0.1	4.6
		M6s	1.4	1.7	8.4	53.2	2.1	4.9	0.5	0.1	4.9
		M7s	1.7	2.2	9.7	52.7	2.4	5.1	0.7	0.1	5.1
		M8s	1.4	1.3	8.6	49.8	2.2	3.8	0.5	0.1	3.8
	Grey, porous travertine	M9s	1.5	2.0	8.7	54.0	2.1	4.8	0.6	0.1	3.8
	Pink ovoid granite	M10s	1.2	1.4	6.7	44.4	1.8	4.4	0.5	0.1	4.4
		M11s	1.5	1.7	7.9	51.4	2.0	5.1	0.6	0.1	5.1
		M12s	1.2	0.7	5.7	50.3	2.0	5.7	0.2	0.0	5.7
		M13s	1.6	1.5	8.9	73.9	2.1	1.4	0.5	0.1	1.4
	Wood	M14s	1.3	1.0	7.1	45.2	1.9	4.8	0.3	0.1	4.8

Figure 5. Heat map of the main impurity elements (wt%) in the biodeposits on the surface of the different rocks, (ICP MS analysis data).

Table 3. The average content (wt%) of the main impurity elements in the biodeposits.

Component	Type of Biodeposit			
	I	II	III	IV
Na ₂ O	2.0 ¹	3.0 ¹	1.7 ¹	1.5 ¹
MgO	10.2 ¹	4.0 ¹	3.8 ¹	1.9 ¹
Al ₂ O ₃	10.9 ¹	16.6 ¹	11.2 ¹	8.5 ¹
SiO ₂	12.3 ²	11.1 ²	29.4 ³	50.6 ³
K ₂ O	7.6 ¹	8.0 ¹	3.9 ¹	2.1 ¹
CaO	1.1 ²	3.0 ²	4.1 ³	4.8 ³
TiO ₂	0.9 ¹	1.8 ¹	0.9 ¹	0.6 ¹
MnO	0.1 ¹	0.2 ¹	0.1 ¹	0.1 ¹
FeO	2.3 ²	1.5 ²	8.7 ³	4.5 ³

Notes: ¹ ICP analysis; ² Electron probe microanalysis; ³ X-ray fluorescence analysis.

Type of biodeposits	Underlying rock	№	Element, mg/kg																																				
			Be	V	Cr	Co	Ni	Cu	Zn	Ga	Rb	Sr	Y	Zr	Nb	Mo	Ag	Sn	Sb	Cs	Ba	La	Ce	Pr	Nd	Sm	Eu	Gd	Tb	Dy	Ho	Er	Tm	Yb	Lu	Hf	W	Th	U
I	Serdobol granite	A 1	1.53	236	253	21.4	77.7	435	459	12.1	89.2	246	18.8	137	9.6	8.91	2.12	27.8	18.7	2.04	982	33.5	64.6	7.91	28.4	5.14	0.91	4.49	0.65	3.56	0.67	1.75	0.27	1.65	0.25	2.98	21.6	9.02	6.21
		A 2	2.48	1450	1350	39.2	123	810	437	24.6	297	375	41.6	267	18.9	18.6	6.84	54.9	12	3.63	2520	81.2	159	18.5	69.3	12	2.03	10.4	1.55	7.91	1.4	3.71	0.51	3.49	0.68	6.21	33.7	20.1	5.03
II	Pudostskii stone	L 1	1.91	838	505	34.3	167	1110	924	29.2	226	342	36.5	655	21.3	14.3	6.97	43.1	8.22	3.5	1430	179	325	27.6	81.2	11.3	1.89	9.9	1.35	7.03	1.26	3.73	0.58	3.35	0.55	13.4	31	20.3	5.13
		L 2	2.57	384	489	40.3	96.6	738	850	27.7	157	337	42.5	123	13.4	17.8	4.23	35.6	21	3.46	1340	74.3	152	17.9	67.2	12.6	2.09	10	1.61	8.65	1.76	4.37	0.63	4.14	0.59	2.46	34.9	21.7	5.28
III	Statuary marble	M1v	1.94	198	248	22.5	70.1	900	224	14.4	95.9	301	24	14.6	4.19	11.2	1.56	20.1	12.2	1.79	1100	38.1	73.9	8.51	32.5	6.14	1.27	5.19	0.85	4.42	0.87	2.25	0.36	2.17	0.35	0.35	15.4	8.99	19.1
	Ruskeala marble	M2v	1.17	223	153	29.7	73.5	1140	926	16.3	92.9	290	31.2	158	10.9	13.5	2.27	42.8	25.2	2.33	1200	48.5	97.1	10.9	43.2	8.45	1.44	6.68	1.03	5.56	1.16	3.02	0.45	2.89	0.42	3.34	22.6	12.7	4.86
	Putilov plate	M3v	1.95	243	443	34.7	115	635	291	17.1	134	327	29.6	20.5	4.92	13.6	4.84	23.9	13.5	2.43	1160	52.9	105	12.1	47	8.84	1.49	7.12	1.06	5.78	1.12	2.87	0.42	2.53	0.39	0.66	27.6	14	5.88
		M4v	1.41	293	327	31.9	128	1010	323	17.5	123	406	31.7	91.7	7.4	15.2	3.79	51.1	32	2.55	1870	51.9	98.7	11.8	44.6	8.51	1.53	7	1.06	5.53	1.08	2.88	0.42	2.68	0.41	1.66	33.6	12.4	4.27
		M5v	2	196	169	28.6	92.2	780	851	17.4	124	400	30.3	50.4	5.71	10.9	3.23	38.8	16.1	2.81	1200	48.9	93.7	11.3	41	7.78	1.5	6.89	1.07	5.77	1.11	2.85	0.4	2.71	0.41	0.77	22.4	11.8	22.2
		M6v	2.12	234	384	26.8	74.8	826	310	15.3	104	342	27.6	43.5	6.68	10.1	2.82	27.4	13.9	2.41	981	41.9	84	9.48	35.7	6.74	1.36	6.1	0.94	4.95	0.98	2.65	0.39	2.42	0.37	0.76	18.1	10.5	5.73
		M7v	1.71	245	143	26.1	87.3	819	876	16.3	109	320	27.4	15.9	6.12	12.6	2.8	27.3	19.2	2.32	1310	45	87.4	10	39	7.45	1.43	6.57	0.99	5.09	0.99	2.66	0.4	2.54	0.39	0.42	24	11.5	4.69
		M8v	1.41	210	129	27.5	74.1	486	1240	15.8	118	366	26.6	51.5	6.89	10.5	2.99	28.6	23.1	2.06	946	43.4	87.2	10.1	38.1	7.02	1.39	6.02	0.95	4.91	0.98	2.58	0.35	2.5	0.36	0.88	22.4	11.1	5.31
	Rapakivi granite	M9v	1.43	173	141	17.6	49.9	604	497	12	83	294	21.4	51.8	7.24	6.88	1.91	24.3	11.8	1.71	775	31.4	64	7.78	28.8	5.54	1.07	4.88	0.73	3.85	0.8	2.12	0.31	1.95	0.31	1.12	11.8	8.12	5.07
		M10v	1.48	225	293	20.7	69.5	466	293	14.2	132	392	23.8	23.2	6.15	8.61	2.81	26.9	13.1	2.34	1090	36.8	73.3	8.62	32.7	5.97	1.25	5.15	0.83	4.23	0.86	2.24	0.38	2.21	0.31	0.56	16.6	9.21	4.31
		M11v	1.43	215	139	19.7	62.4	450	878	15.4	109	371	27	48.7	8.38	7.94	2.81	25.7	11.4	2.38	1060	40.7	83.1	9.55	35.8	7.04	1.36	6.18	0.94	5.1	1.02	2.67	0.37	2.26	0.36	1	17	11.9	4.52
		M12v	1.83	221	157	26.3	69.8	645	680	17.1	80.2	310	25.8	162	12.2	9.25	2.13	31.8	17.3	1.95	924	38.6	78.7	9	34.8	6.7	1.4	5.92	0.9	4.79	0.97	2.57	0.38	2.19	0.33	3.89	17.9	10.9	4.35
	Wood	M13v	1.67	189	91.6	25.9	70	571	1110	16.4	120	361	27.6	24.4	5.88	9.08	2.84	27.7	14.2	2.62	1180	42.1	83.3	9.69	36.1	6.74	1.36	6.06	0.89	5.04	0.96	2.75	0.36	2.51	0.38	0.38	18.3	11.1	7.67
	Wood	M14v	1.61	203	110	23.1	61.1	602	971	15.9	100	314	25.8	29.7	5.23	7.86	2.63	22.9	14.4	2.12	885	40.4	81.9	9.82	36	6.82	1.31	5.94	0.88	4.93	0.95	2.5	0.37	2.24	0.34	0.71	15.7	11.1	4.09
IV	Statuary marble	M1s	1.39	106	83.3	14.7	40.2	104	405	12.1	73.9	173	18.6	184	9.12	3.46	0.1	8.56	4	1.49	629	27.4	54.6	6.33	24.8	4.69	1.01	4.11	0.53	3.32	0.65	1.84	0.24	1.8	0.26	4.42	9.86	6.64	1.92
	Ruskeala marble	M2s	1	142	89	21.1	45.7	182	592	13.9	67.5	192	23.9	217	10.2	9.77	0.1	16.8	6.55	1.49	617	32.3	67.6	7.8	32	6	1.16	5.21	0.69	4.3	0.84	2.32	0.32	2.06	0.33	5.43	11.4	8.45	2.89
	Putilov plate	M3s	1.33	91.5	97.4	15.7	47.4	200	512	11.9	78.1	149	23.3	166	9.46	4.5	0.1	6.7	3.55	1.87	690	28.2	54.6	6.39	25.7	5.36	0.93	4.52	0.62	3.87	0.76	2.18	0.3	2.13	0.31	4.29	12.5	8.52	2.02
		M4s	1.35	162	107	25	47.7	206	928	15.5	69.3	200	27.4	264	12.2	5.29	0.1	17.1	8.32	1.51	741	36.7	78.8	8.57	35.4	6.82	1.23	6.09	0.88	5.08	0.91	2.66	0.39	2.46	0.37	6.79	12.8	11.2	2.36
		M5s	1.31	91.9	66	14.7	33.7	114	414	12.5	85.3	156	24.8	245	8.84	2.91	0.1	10.7	2.67	1.9	646	29.9	61.8	7.03	28.2	5.4	0.98	4.54	0.65	4.13	0.79	2.3	0.38	2.46	0.4	5.65	8.85	9.04	2.47
		M6s	1.62	115	95.8	16.2	41	126	479	13.1	83.2	187	22.9	254	9.54	4.3	0.1	10.2	5.92	1.73	696	27.2	55.3	6.36	26.7	5.21	1.16	4.42	0.65	4.04	0.75	2.19	0.32	2.3	0.32	6.09	16.4	7.34	2.05
		M7s	1.18	90.3	69.2	13.5	32.1	134	458	11.7	76.5	154	20.1	184	8.32	3.71	0.1	10.3	3.9	1.69	691	45.4	83.9	9.66	37.1	6.58	1.02	5.64	0.64	3.75	0.69	1.98	0.27	1.69	0.27	4.24	9.83	17.4	3.56
		M8s	1.21	106	93.6	15.4	44.4	209	619	12.1	78.4	166	20.2	182	10.5	4.81	0.1	10.5	4.57	1.68	706	25.7	54.3	6.62	25	5.17	0.97	4.58	0.58	3.6	0.76	1.91	0.31	1.81	0.25	4.47	12.6	6.98	1.87
	Pudostskii stone	M9s	1.42	109	81.3	15.7	41.3	189	497	12.4	69.4	187	19.8	231	9.35	3.62	0.1	13.4	5.24	1.49	683	27.4	55.3	6.52	26.1	4.89	1.05	4.51	0.57	3.61	0.7	1.98	0.28	1.96	0.27	5.5	9.5	7.9	1.82
	Rapakivi granite	M10s	1.39	84.7	63.9	13.1	34.6	172	414	10.9	70.6	153	18.8	164	9.23	3.12	0.1	9.84	4.06	1.49	582	24.5	50	5.62	23.1	4.56	0.93	3.74	0.53	3.59	0.64	1.75	0.26	1.98	0.27	4.23	8.07	6.75	3.86
		M11s	1.8	96.2	81.6	16	53	146	461	12.1	76.8	173	20.3	235	9.6	4.16	0.1	12.5	4.84	1.79	671	29.2	61.9	7.26	28	5.76	1	4.97	0.63	3.7	0.69	2.17	0.31	1.94	0.27	5.88	11.1	8.74	5.93
		M12s	1.22	30.7	30.8	4.21	19.6	67.5	294	7.98	66.4	112	11.6	99.8	4.16	1.71	0.1	3.49	0.78	1.15	396	13.6	26.9	3.14	11.6	2.36	0.6	1.92	0.28	2.08	0.39	1.31	0.26	1.79	0.32	2.67	3.61	3.95	1.13
	Wood	M13s	1.28	90.2	69.1	14.1	32.9	133	393	9.66	62.2	133	16.5	140	7.69	3.93	0.1	7.49	1.88	1.26	458	24.4	49.4	5.72	22.9	4.35	0.76	3.64	0.47	2.91	0.6	1.66	0.27	1.61	0.25	3.22	10.5	7.06	2.63
	Wood	M14s	1.51	62.2	57	9.32	31.4	111	696	9.03	67.5	147	15.5	153	6.79	2.29	0.1	12.8	5.06	1.28	639	20.8	39.7	4.74	18.1	3.5	0.74	3.19	0.44	2.8	0.54	1.57	0.22	1.37	0.22	3.6	9.71	6	1.86

Figure 6. Heat map of trace impurity elements (mg/kg) in the biodeposits on the surface of the different rocks (1 mg/kg = 10⁻⁵ wt%).

Table 4. The average content of the trace impurity elements (mg/kg)¹ in the biodeposits (ICP MS analysis data).

Element	Type of Biodeposits			
	I	II	III	IV
Be	2.0	2.0	1.6	1.4
V	843.0	611.0	219.1	98.4
Cr	801.5	497.0	209.1	77.5
Co	30.3	37.3	25.8	14.9
Ni	100.3	131.8	78.4	38.9
Cu	622.5	924.0	709.6	149.5
Zn	448.0	887.0	676.4	511.6
Ga	18.3	28.5	15.8	11.8
Rb	193.1	191.5	108.9	73.2
Sr	310.5	339.5	342.4	163.0
Y	30.2	39.5	27.1	20.3
Zr	202.0	389.0	56.1	194.2
Nb	14.2	17.3	7.0	8.9
Mo	13.7	16.0	10.5	4.1
Ag	4.5	5.6	2.8	0.1
Sn	41.3	39.3	29.9	10.7
Sb	15.3	14.6	16.9	4.4
Cs	2.8	3.5	2.3	1.6
Ba	1751.0	1385.0	1120.1	631.8
La	57.3	126.6	42.9	28.0
Ce	111.8	238.5	85.1	56.7
Pr	13.2	22.7	9.9	6.5
Nd	48.8	74.2	37.5	26.1
Sm	8.6	11.9	7.1	5.0
Eu	1.5	2.0	1.4	1.0
Gd	7.5	9.9	6.1	4.4
Tb	1.1	1.5	0.9	0.6
Dy	5.7	7.8	5.0	3.6
Ho	1.0	1.5	1.0	0.7
Er	2.7	4.0	2.6	2.0
Tm	0.4	0.6	0.4	0.3
Yb	2.6	3.7	2.4	1.9
Lu	0.5	0.6	0.4	0.3
Hf	4.6	7.9	1.2	4.7
W	27.6	32.9	20.2	10.5
Th	14.6	21.0	11.1	8.3
U	5.6	5.2	7.3	2.6

Note: ¹ 1 wt% = 10,000 mg/kg.

The various types of biodeposits are characterized by an identical set of inorganic elements but differ in their quantity.

The content of the main impurity elements Na, Al, Ti, and Mn is higher in biodeposits with a predominance of lichens (type II) in comparison with other types of biodeposits (Figure 5, Table 3). The content of silicon and calcium is significantly higher in mosses and, especially, in the primary soil under the moss cover. Iron is contained in the vegetative part of mosses and the underlying soil (in type III and IV of biodeposits) in a higher concentration than in type I and II of biodeposits. But in contrast to calcium and silicon, the iron content is higher in the vegetative part of mosses (type III of biodeposits), and not in the primary soil (type IV of biodeposits).

Trace elements are found in higher concentrations in biodeposits dominated by fungi and algae, as well as lichens (type I and II of biodeposits) than in the primary soil with a moss cover (type III and IV of biodeposits) (Figure 6, Table 4). Lichen-dominated biodeposits (type II) are characterized by the accumulation of most trace impurity elements in the highest concentrations. The concentration of most trace impurity elements was higher in the vegetative part of mosses (type III of biodeposits) as compared to the primary soil under them (type IV of biodeposits). The exceptions were Zr, Nb, Hf, the concentration of which was higher in the primary soil.

No relationship was found between the elemental compositions of the underlying rock and biodeposits (Figures 5 and 6). No significant differences were observed when comparing biodeposits on silicate and carbonate rocks in terms of the content of calcium and silicon, as well as when comparing the primary soil on monuments made of wood and stone. Only the content of Si in the vegetative part of moss (III type) sampled from the surface of stone monuments was higher than its content in moss sample taken from the surface of the wooden monument. In primary soil (IV type) Si content did not differ significantly between all samples. Similar data was obtained for calcium: its content in mosses on a wooden monument was no more than 4-6 times lower than on the surface of a stone, and in the primary soil was almost equal.

As shown by the example of white calcite homogeneous marble (Table 5), the content of the main impurity elements in biodeposits and dust is significantly higher (not less than an order of magnitude) than in the bedrock. The concentrations of these elements in biodeposits and dust are of the same order of magnitude. At the same time, a trend can be seen: the concentration of impurity elements in the dust is closer to the concentrations in the primary soil (in comparison with the vegetative part of mosses).

Table 5. Content of the main impurity elements (wt%) in Carrara marble and deposits (dust, moss and primary soil) on its surface.

Component	Marble	Dust	Biodeposits	
			Sam.M1v	Sam.M1s
Na ₂ O	0.01 ²	3.0 ¹	1.6 ¹	1.6 ¹
MgO	0.17 ²	4.0 ¹	3.7 ¹	2.0 ¹
Al ₂ O ₃	0.088 ²	16.6 ¹	9.9 ¹	9.1 ¹
SiO ₂	0.01 ²	11.1 ²	36.5 ³	50.7 ³
K ₂ O	0.009 ²	8.0 ¹	3.5 ¹	2.3 ¹
CaO	99.0 ²	3.0 ²	4.3 ³	5.2 ³
TiO ₂	0.066 ²	1.8 ¹	0.8 ¹	0.6 ¹
MnO	0.01 ²	0.2 ¹	0.13 ¹	0.1 ¹
FeO	0.019 ²	1.5 ²	8.2 ³	5.2 ³

Notes: ¹ ICP analysis; ² Electron probe microanalysis; ³ X-ray fluorescence analysis.

Analysis of the studied elemental compositions by the method of principal components (PCA) leads to the formation of four clusters corresponding to all types of analyzed biodeposits and makes it possible to assess the degree of difference in their compositions (Figures 7 and 8).

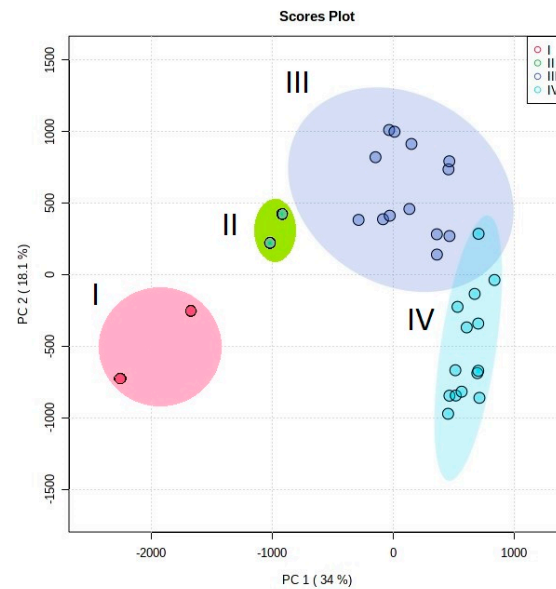


Figure 7. Results of principal component analysis (PCA) of the main impurity elements in biodeposits on the surface of stone: I—biofilms with a predominance microscopic fungi and algae; II—biofilms with a predominance lichens; III—vegetative biomass of the moss; IV—primary soil under the moss cover. The main contribution to the statistical model for PC 1 is made by TiO_2 , Na_2O , Al_2O_3 and for PC 2 by MgO , K_2O , and MnO .

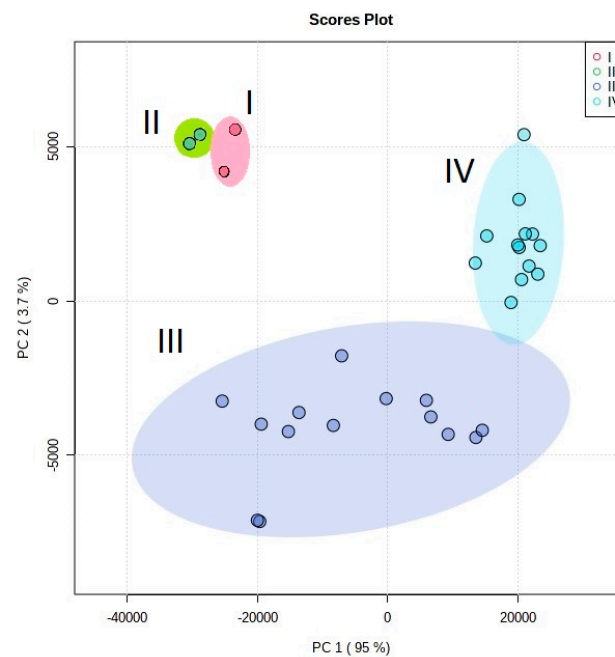


Figure 8. Results of PC analysis of the trace elements in biodeposits on the surface of stone: I—biofilms with a predominance microscopic fungi and algae; II—biofilms with a predominance lichens; III—vegetative biomass of the moss; IV—primary soil under the moss cover. The main contribution to the statistical model for PC 1 is made by Eu , Sm , Pr , Nd , Ce , Gd , Zn , Rb , Dy , Sn and for PC 2 by Lu , Sr , Y , Pb , Ge , Ag , Cs , Ba , Zr , Ni .

Unlike the I and II types, macrodeposits of moss (III and the IV types) can be analyzed at the species level, which can also be important when assessing the specificity of the accumulation of elements by organisms. Moss samples (type III of biodeposits), represented by only one species, totaled a representative set (more than three samples) for the species *C. purpureus*, *B. salebrosum*, and *S. apocarpum*. Analysis of the distribution of the main impurity elements depending on the belonging of the mosses to specific species showed significant differences in the accumulation of silicon (Figure 9). The amount of Si in the biomass increased in the series *C. purpureus*, *B. salebrosum*, *S. apocarpum*.

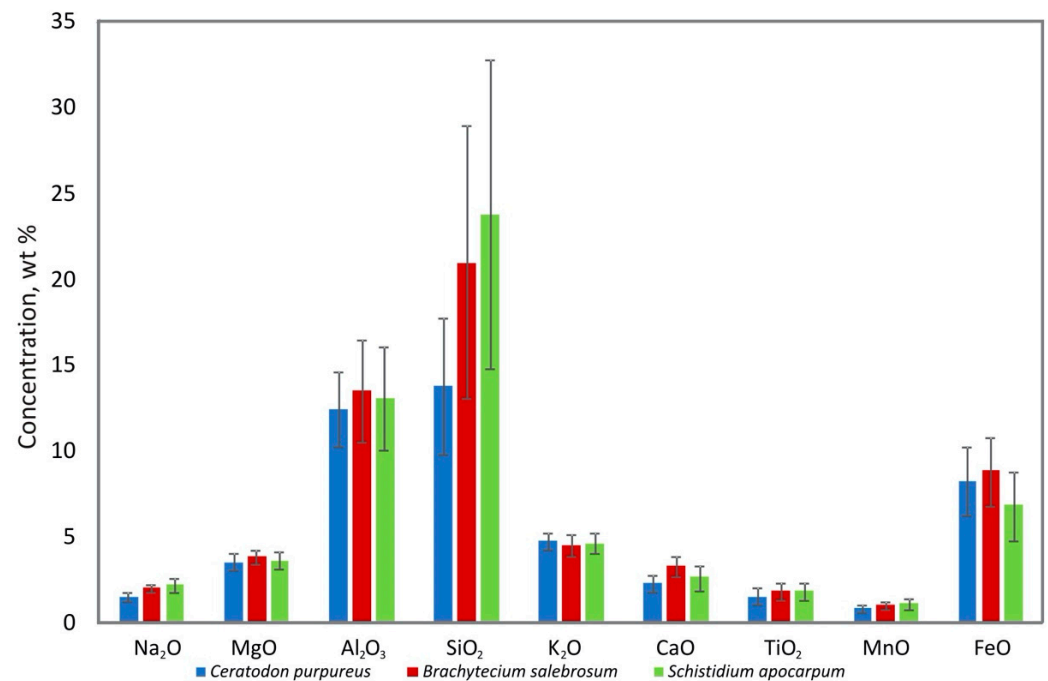


Figure 9. Content of the main impurity elements (wt%) in mosses of different species composition.

4. Discussion

The obtained results allow to make a comparative analysis of the influence of the bedrock, the environment, and the species composition of microorganisms on the elemental composition of biodeposits and restore (at a model level) the picture of the input and selective accumulation of elements in biodeposits on the surface of the different rocks in an outdoor environment.

4.1. The Influence of the Bedrock, the Environment, and the Species of Microorganisms on the Elemental Composition of Biodeposits

No significant differences in the elemental composition of biodeposits depending on the underlying substrate were revealed (Figures 5 and 6). For example, this is clearly seen when comparing biodeposits on silicate and carbonate rocks in terms of the content of calcium and silicon (Figure 10).

This is also confirmed by the closeness of the elemental compositions of biodeposits on the surface of wood and rocks (Figures 5 and 6).

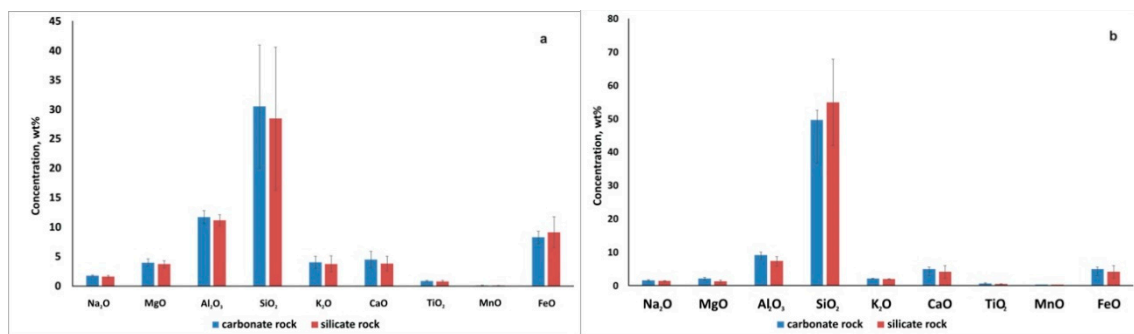


Figure 10. Comparison of average concentrations (wt%) of the main impurity elements in biodeposits on carbonate and silicate rocks: (a)—in mosses (III type of biodeposits); (b)—primary soil under them (IV type of biodeposits).

Accordingly, it can be assumed that the contribution of the underlying rock to the elemental composition of the studied biodeposits is significantly less than that of the environment. This conclusion is also supported by the fact that the content of impurity elements in the rocks is at least an order of magnitude lower than in the deposits on its surface (Table 5). There is also evidence of that in the results of a comparison of the elemental composition of type III and IV biodeposits (mosses and primary soil formed under them). The results of cluster analysis (Figures 7 and 8) indicate the decisive role of the taxonomic affiliation of organisms in the pattern of the selective accumulation in biodeposits of elements transferred to the stone surface predominantly from the environment. The elemental composition of type I biodeposits (with a predominance of fungi and algae) differs significantly from type II biodeposits (with a predominance of lichens) only in terms of the main impurity elements (Figure 7). Differences in the elemental composition of biodeposits of types III and IV (the upper vegetation part of the mosses and the lower layer of the primary soil) are more pronounced for the trace elements (Figure 8).

Thus, the results of the comparative analysis showed that the elemental composition of investigated biodeposits on the surface of outdoor stone is mainly controlled by the environment and the composition of microorganism species inhabiting stone surface (at the level of large taxa). The specificity in the accumulation of elements at the species level (as shown by the example of mosses) also takes place, but it is not as contrasting as when comparing large taxa.

4.2. The Picture of the Input and Accumulation of Elements in Biodeposits on the Surfaces of Stone Monument in Outdoor Environment (at a Model Level)

The obtained results and knowledge gathered previously by us and other researchers allow us to recreate at a model level the picture of the input and selective accumulation of elements in biodeposits on the stone surfaces. The lack of relationships between the elemental composition of biodeposits and underlying rocks can be explained by assuming that a significant contribution to the elemental composition of biodeposits is made by leaching under the action of microbial metabolites of mineral grains present in biofouling and young soils. According to our data, the mineral composition of the grains in the biodeposits is determined by the mineral composition of all the rocks from which the monuments of the necropoleis are made and varies little from monument to monument. The results of our long-term monitoring indicate intensive weathering of the stone materials of the necropoleis monuments [41]. Grains of various minerals entering the environment can be picked up by wind currents, mixed and have a tendency to be averaged over all the stone monuments of the necropoleis.

Of course, elements turn out to be on the surface of monuments and without the participation of wind, for example, in the form of aerosols directly from the air during acid rains and fogs [41]. However, the mineral composition of grains in biodeposits on the surface of monuments, which was determined by us, can be formed only with the participation of wind flows. Thus, all the results obtained indicate that elements enter

the biodeposits on the stone surface (biofouling and primary soils) mainly from the environment. This conclusion correlates with a number of other researches [40,58].

The differences in the elemental composition of the studied biodeposits via cluster analysis (Figures 7 and 8) can be explained using the well-known mechanisms of accumulation of elements by the microbial community. Biodeposits of types I and II (in which the fungal component dominates) are characterized by a greater ability to accumulate elements (with the exception of iron, calcium, and silicon prevailing in mosses). This can be explained by the fact that fungal biomass is more capable of sorption of cations due to the large number of highly active functional amino groups in chitin [59], the presence of extracellular melanins [31], as well as due to the significant contribution of the cell wall to the total biomass of fungi [19]. Because sorption is a surface reaction, the biosorption potential of a biosorbent depends on its surface area and its polarity. We can say that the performance of a biosorbent depends on the ionic state of the biomass. Thus, fungal biomass received much attention as a biosorbent because of the presence of a high percentage of cell-wall material, which increases the variety of functional groups involved in metal binding [60]. Additionally, it is impossible to exclude the formation of complexes occurring due to extracellular ion exchange reactions and intracellular accumulation of elements due to their binding by specific proteins and organic acids.

Another possible reason for determining the composition of ions in biodeposits is the extracellular formation of poorly soluble salts of oxalic acid, primarily calcium oxalates (Figure 11). Oxalic acid is excreted by many species of lichen [18]. Besides, among the fungi revealed in the studied biodeposits, the species of genus *Penicillium* have an intense ability for extracellular production of organic acids, including oxalic acid. Some other species, for example, *T. viride*, *A. alternata*, *A. pullulans*, are also capable of acid production activity under certain conditions [61,62].

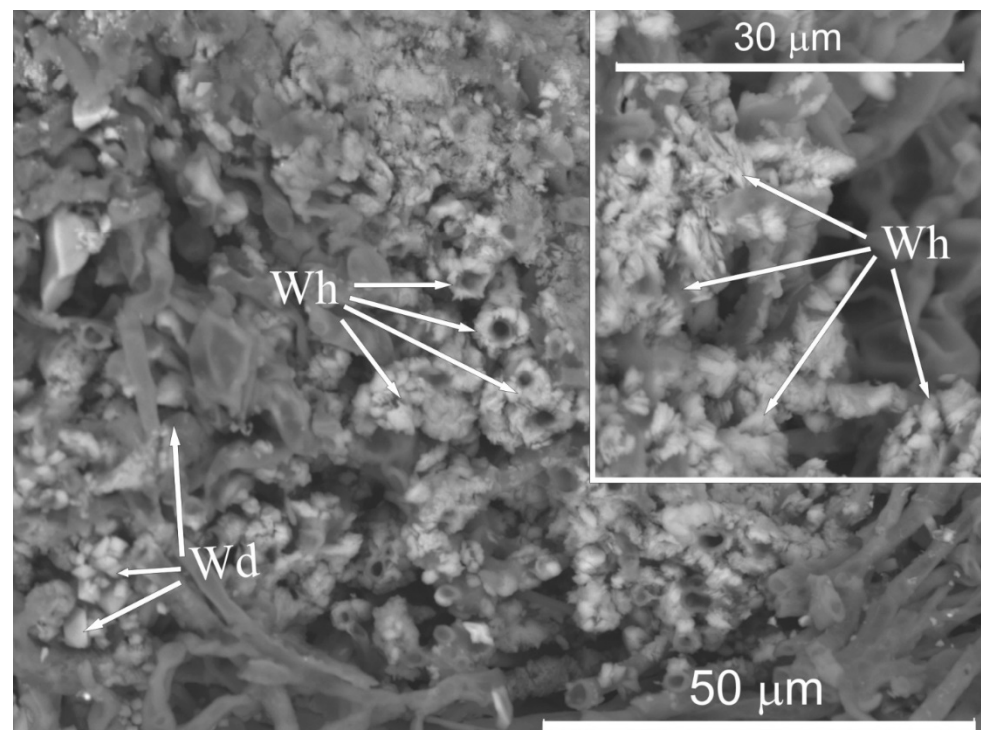


Figure 11. SEM-images of calcium oxalate crystals in lichen dominated biodeposits on the surface of homogeneous calcite marble: dipyrnidal crystals of weddellite (Wd) and lamellar crystals of whewellite (Wh).

Differences in the content of the main impurity elements of biodeposits of types I and II were clear (Figure 7), and they were really absent for trace impurity elements

(Figure 8). Perhaps this is due to the fact that for the main impurity elements the role of the mechanism of intracellular accumulation is more significant than for the trace impurity elements, and organisms can exhibit greater selectivity and variability in the accumulation of these elements.

Mosses, regardless of their species, are less likely to accumulate most elements, with the exception of iron, calcium, and silicon. We believed that in mosses, the extracellular fraction of metals is usually easily exchanged and tends to reflect current environmental conditions and sporadic pollution by many elements. The intracellular fraction is the result of the integration of metals over a longer period of time and thus characterizes the average situation in the environment [63]. The revealed regularity can be explained if we assume that the elements present in the highest concentrations (iron, calcium and silicon) accumulate in mosses intracellularly, and the elements with lower concentrations mainly bind extracellularly.

The primary soil under mosses (type IV biodeposits) contains the lowest concentrations of elements, with the exception of Ca, Si, Hf, Nb, and Zr. Kłos et al. [64] proposed two mechanisms for the transfer of metals from the soil to mosses: transport of elements with raised dust and their diffusion through aqueous solutions. It can be assumed that the elements transferred by aqueous solutions into the plant biomass of mosses come mainly from primary soil, to where they get from mineral grains from the environment and, to a lesser extent, from the underlying rocks. Ca and Si, probably, cannot be consumed by mosses in such high concentrations and therefore dominate in primary soil. As for the trace impurity elements Hf, Nb, and Zr, the probable reason for their predominant accumulation in the primary soil, rather than in the vegetative part of the moss, is probably due to the poor bioavailability of these elements for the plant. Some evidence suggests that only a small fraction of zirconium is available for plant uptake, because of strong binding with organic and inorganic ligands in soils [65].

5. Conclusions

The studied biodeposits formed by living organisms and the extracellular products of their metabolism on the stone surface in outdoor conditions (biofouling, primary soils) contain numerous elements (from Be to REE), the concentration of which varies substantially.

The element composition of biodeposits is controlled mainly by the environment and the species composition of microorganisms inhabiting stone (at the level of large taxa). The contribution to the elemental composition from leaching (under the action of microbial metabolites) of mineral grains, which enter biodeposits from the environment, is more significant than that of the underlying rocks.

The picture of the input and selective accumulation of elements in biodeposits on the stone surfaces (recreated at a model level) allows us to explain the insignificant contribution of the underlying rocks to the elemental composition of biodeposits only if we take into account the essential role of wind flows in the formation of the biodeposit mineral component.

The obtained results significantly expand the understanding of the chemical composition of the medium in which oxalate crystallization occurs in biofilms and contribute to the development of ideas about microbial biomineralization mechanisms.

Author Contributions: Conceptualization (D.Y.V., O.V.F.-K. and K.V.S.); investigation (V.V.M., M.S.Z., A.V.R. and A.R.I.); methodology (K.V.S., M.S.Z., D.Y.V. and O.V.F.-K.); visualization (K.V.S., A.V.R., A.R.I. and M.S.Z.); writing—original draft (K.V.S.); writing—review & editing (D.Y.V. and O.V.F.-K.); translation to English (A.V.R.). All authors have read and agreed to the published version of the manuscript.

Funding: The research was funded by the Russian Science Foundation (grant 19–17–00141).

Acknowledgments: The authors would like to thank E.N. Kotelnikova, Yu.L. Kretser, L.E. Kurbatova for consultations provided during the preparation of the article. The laboratory researches were carried out: SEM investigations—in the “Resource Center Microscopy and Microanalysis (RCMM)”

of Saint Petersburg State University; XRD measurements—in the X-ray Diffraction Centre of Saint Petersburg State University; ICP MS—in the Central analytical laboratory of Karpinsky All-Russian Geological Research Institute; XRFS—in the Fersman Environmental Geochemistry Laboratory (Herzen State Pedagogical University of Russia).

Conflicts of Interest: The authors declare no conflict of interest.

References

- Kurakov, A.V.; Somova, N.G.; Ivanovskii, R.N. Micromycetes populating limestone and red brick surfaces of the Novodevichii convent masonry. *Microbiology* **1999**, *68*, 273–282.
- Warscheid, T.; Braams, J. Biodeterioration of stone: A review. *Int. Biodeterior. Biodegradation* **2000**, *46*, 343–368. [[CrossRef](#)]
- Salvadori, O.; Mucchia, A.C. The Role of Fungi and Lichens in the Biodeterioration of Stone Monuments. *Open Conf. Proc. J.* **2016**, *7*, 39–54. [[CrossRef](#)]
- Misra, J.K.; Tewari, J.P.; Deshmukh, S.K.; Vágvölgyi, C. Microfungi from deteriorated materials of cultural heritage. In *Fungi from Different Substrates*; CRC Press: Boca Raton, FL, USA; Taylor and Francis Group: Abingdon, UK, 2015; pp. 144–158.
- Di Martino, P. What about Biofilms on the Surface of Stone Monuments? *Open Conf. Proc. J.* **2016**, *6*, 14–28. [[CrossRef](#)]
- Girbal, J.; Prada, J.L.; Rocabayera, R.; Argemi, M. Dating of Biodeposits of Oxalates at the Arc De Berà in Tarragona, Spain. *Radiocarbon* **2001**, *43*, 637–645. [[CrossRef](#)]
- Gadd, G.M. Fungal Production of Citric and Oxalic Acid: Importance in Metal Speciation, Physiology and Biogeochemical Processes. *Adv. Microb. Physiol.* **1999**, *41*, 47–92. [[CrossRef](#)]
- Sayer, J.A.; Gadd, G.M. Binding of cobalt and zinc by organic acids and culture filtrates of *Aspergillus niger* grown in the absence or presence of insoluble cobalt or zinc phosphate. *Mycol. Res.* **2001**, *105*, 1261–1267. [[CrossRef](#)]
- Gadd, G.M. Geomycology: Biogeochemical transformations of rocks, minerals, metals and radionuclides by fungi, bioweathering and bioremediation. *Mycol. Res.* **2007**, *111*, 3–49. [[CrossRef](#)]
- Gadd, G.M. *Fungi in Bioremediation*; Cambridge University Press: Cambridge, UK, 2001; pp. 359–382. [[CrossRef](#)]
- Frank-Kamenetskaya, O.V.; Ivanyuk, G.Y.; Zelenskaya, M.S.; Izatulina, A.R.; Kalashnikov, A.O.; Vlasov, D.Y.; Polyanskaya, E.I. Calcium Oxalates in Lichens on Surface of Apatite-Nepheline Ore (Kola Peninsula, Russia). *Minerals* **2019**, *9*, 656. [[CrossRef](#)]
- Purvis, O.W.; Pawlik-Skowrońska, B.; Cressey, G.; Jones, G.C.; Kearsley, A.; Spratt, J. Mineral phases and element composition of the copper hyperaccumulator lichen *Lecanora polytropa*. *Miner. Mag.* **2008**, *72*, 607–616. [[CrossRef](#)]
- Monte, M. Oxalate film formation on marbles specimens caused by fungus. *J. Cult. Herit.* **2003**, *4*, 255–258. [[CrossRef](#)]
- Adamo, P. Weathering of rocks and neogenesis of minerals associated with lichen activity. *Appl. Clay Sci.* **2000**, *16*, 229–256. [[CrossRef](#)]
- Bonaventura, M.D.G.M.P.D. Microbial Formation of Oxalate Films on Monument Surfaces: Bioprotection or Biodeterioration? *Geomicrobiol. J.* **1999**, *16*, 55–64. [[CrossRef](#)]
- Sazanova, K.V.; Vlasov, D.Y.; Osmolovskay, N.G.; Schiparev, S.M.; Rusakov, A.V. Significance and regulation of acids production by rock-inhabited fungi. In *Biogenic-Abiogenic Interactions in Natural and Anthropogenic Systems*; Frank-Kamenetskaya, O.V., Panova, E.G., Vlasov, D.Y., Eds.; Springer International Publishing: Cham, Switzerland, 2016; pp. 379–392. [[CrossRef](#)]
- Sazanova, K.V.; Frank-Kamenetskaya, O.V.; Vlasov, D.Y.; Zelenskaya, M.S.; Vlasov, A.D.; Rusakov, A.V.; Petrova, M. Carbonate and Oxalate Crystallization by Interaction of Calcite Marble with *Bacillus subtilis* and *Bacillus subtilis*-*Aspergillus niger* Association. *Crystals* **2020**, *10*, 756. [[CrossRef](#)]
- Vlasov, D.Y.; Frank-Kamenetskaya, O.V.; Zelenskaya, M.S.; Sazanova, K.V.; Rusakov, A.D.; Izatulina, A.R. The use of *Aspergillus niger* in modeling of modern mineral formation in lithobiotic systems. In *Aspergillus Niger: Pathogenicity, Cultivation and Uses*; Baughan, E., Ed.; Nova Science Publishers: New York, NY, USA, 2020; pp. 1–123.
- Siddiquee, S.; Rovina, K.; Al Azad, S. Heavy Metal Contaminants Removal from Wastewater Using the Potential Filamentous Fungi Biomass: A Review. *J. Microb. Biochem. Technol.* **2015**, *7*, 384–393. [[CrossRef](#)]
- Wells, J.M.; Brown, D.H. Ionic control of intracellular and extracellular Cd uptake by the moss *Rhytidiadelphus squarrosus* (Hedw.) Warnst. *New Phytol.* **1990**, *116*, 541–553. [[CrossRef](#)]
- Shakya, K.; Chettri, M.K.; Sawidis, T. Impact of Heavy Metals (Copper, Zinc, and Lead) on the Chlorophyll Content of Some Mosses. *Arch. Environ. Contam. Toxicol.* **2008**, *54*, 412–421. [[CrossRef](#)]
- Mukhopadhyay, M.; Noronha, S.B.; Suraiashkumar, G.K. A review on experimental studies of biosorption of heavy metals by *Aspergillus niger*. *Can. J. Chem. Eng.* **2011**, *89*, 889–900. [[CrossRef](#)]
- Tian, D.; Jiang, Z.; Jiang, L.; Su, M.; Feng, Z.; Zhang, L.; Wang, S.; Li, Z.; Hu, S. A new insight into lead (II) tolerance of environmental fungi based on a study of *Aspergillus niger* and *Penicillium oxalicum*. *Environ. Microbiol.* **2019**, *21*, 471–479. [[CrossRef](#)]
- Chandran, S.C.; Shijith, K.V.; Vipin, K.V.; Augusthy, A.R. Study on heavy metals toxicity biomarkers in *Aspergillus niger*. *IJAPBC* **2014**, *3*, 458–464.
- Biosorption of Mercury by Biomass of Filamentous Algae *Spirogyra* Species. *J. Biol. Sci.* **2006**, *6*, 695–700. [[CrossRef](#)]
- Okuo, J.M.; Sanni, S.; Aigbedion, S. Selective Biosorption of Heavy Metal Ions from Aqueous Solutions by Pre-Treated Nigerian Fresh Water Algae. *Trends Appl. Sci. Res.* **2006**, *1*, 83–90. [[CrossRef](#)]

27. González, A.G.; Pokrovsky, O. Metal adsorption on mosses: Toward a universal adsorption model. *J. Colloid Interface Sci.* **2014**, *415*, 169–178. [[CrossRef](#)] [[PubMed](#)]
28. Rola, K. Insight into the pattern of heavy-metal accumulation in lichen thalli. *J. Trace Elem. Med. Biol.* **2020**, *61*, 126512. [[CrossRef](#)]
29. Dhankhar, R.; Hooda, A. Fungal biosorption—an alternative to meet the challenges of heavy metal pollution in aqueous solutions. *Environ. Technol.* **2011**, *32*, 467–491. [[CrossRef](#)]
30. Gadd, G.M. Heavy metal accumulation by bacteria and other microorganisms. *Cell. Mol. Life Sci.* **1990**, *46*, 834–840. [[CrossRef](#)]
31. Fogarty, R.V.; Tobin, J.M. Fungal melanins and their interactions with metals. *Enzym. Microb. Technol.* **1996**, *19*, 311–317. [[CrossRef](#)]
32. Chen, J.; Blume, H.-P.; Beyer, L. Weathering of rocks induced by lichen colonization—A review. *Catena* **2000**, *39*, 121–146. [[CrossRef](#)]
33. Carter, D.; Arocena, J. Soil formation under two moss species in sandy materials of central British Columbia (Canada). *Geoderma* **2000**, *98*, 157–176. [[CrossRef](#)]
34. Sayer, J.A.; Gadd, G.M. Solubilization and transformation of insoluble inorganic metal compounds to insoluble metal oxalates by *Aspergillus niger*. *Mycol. Res.* **1997**, *101*, 653–661. [[CrossRef](#)]
35. Bargagli, R.; Monaci, F.; Borghini, F.; Bravi, F.; Agnorelli, C. Mosses and lichens as biomonitors of trace metals. A comparison study on Hypnum cupressiforme and Parmelia caperata in a former mining district in Italy. *Environ. Pollut.* **2002**, *116*, 279–287. [[CrossRef](#)]
36. Chakraborty, S.; Paratkar, G.T. Biomonitoring of Trace Element Air Pollution Using Mosses. *Aerosol Air Qual. Res.* **2006**, *6*, 247–258. [[CrossRef](#)]
37. Szczepaniak, K.; Biziuk, M. Aspects of the biomonitoring studies using mosses and lichens as indicators of metal pollution. *Environ. Res.* **2003**, *93*, 221–230. [[CrossRef](#)]
38. Harmens, H.; Norris, D.A.; Koerber, G.; Buse, A.; Steinnes, E.; Rühling, Å. Temporal trends in the concentration of arsenic, chromium, copper, iron, nickel, vanadium and zinc in mosses across Europe between 1990 and 2000. *Atmos. Environ.* **2007**, *41*, 6673–6687. [[CrossRef](#)]
39. Kłos, A.; Rajfur, M.; Šrámek, I.; Wacławek, M. Use of Lichen and Moss in Assessment of Forest Contamination with Heavy Metals in Praded and Glacensis Euroregions (Poland and Czech Republic). *Water Air Soil Pollut.* **2011**, *222*, 367–376. [[CrossRef](#)] [[PubMed](#)]
40. Jiang, Y.; Fan, M.; Hu, R.; Zhao, J.; Wu, Y. Mosses Are Better than Leaves of Vascular Plants in Monitoring Atmospheric Heavy Metal Pollution in Urban Areas. *Int. J. Environ. Res. Public Health* **2018**, *15*, 1105. [[CrossRef](#)]
41. Frank-Kamenetskaya, O.V.; Vlasov, D.Y.; Rytikova, V.V. (Eds.) *The Effect of the Environment on Saint Petersburg's Cultural Heritage. Results of Monitoring the Historical Necropolis Monuments*; Springer Nature Switzerland AG: Cham, Switzerland, 2019; 188p.
42. Sazanova, K.V.; Zelenskaya, M.S.; Bobir, S.Y.; Vlasov, D.Y. Micromycetes in the biofilms on stone monuments of Saint Petersburg. *Micol. Phytopathol. (Mycol. Phytopathol.)* **2020**, *54*, 329–339. [[CrossRef](#)]
43. Ellis, M.B. *Dematiaceous Hyphomycetes*. Kew, Surrey; Commonwealth Mycological Institute: London, UK, 1971; 608p.
44. Ellis, M.B. *More Dematiaceous Hyphomycetes*. Kew, Surrey; Commonwealth Mycological Institute: London, UK, 1976; 507p.
45. De Hoog, G.S.; Guarro, J. *Atlas of Clinical Fungi*; CBS: Baarn, The Netherlands, 1995; 1160p.
46. De Hoog, G.S.; Hermanides-Nijhof, E.J. Survey of the black yeasts and allied fungi. *Stud Mycol.* **1977**, *15*, 178–223.
47. Available online: <http://www.indexfungorum.org/NAMES/NAMES.asp> (accessed on 20 November 2020).
48. Graham, L.E.; Wilcox, L.W. *Algae*; Prentice Hall: Upper Saddle River, NJ, USA, 2000; 650p.
49. Guiry, M.D.; Guiry, G.M. *AlgaeBase*; World-Wide Electronic Publication; National University of Ireland: Galway, Ireland; Available online: <http://www.algaebase.org> (accessed on 20 July 2020).
50. Nordin, A.; Moberg, R.; Tønsberg, T.; Vitikainen, O.; Dalsätt, Å.; Myrdal, M.; Snitting, D.; Ekman, S. *Santesson's Checklist of Fennoscandian Lichen-forming and Lichenicolous Fungi*; Version 29; Museum of Evolution, Uppsala University: Uppsala, Sweden, 2011; Available online: <http://130.238.83.220/santesson/home.php> (accessed on 15 November 2020).
51. Foucard, T. *Svenska Skorplavar och Svampar som Växer på dem*; Interpublishing: Stockholm, Sweden, 2001; 392p.
52. Smith, C.W.; Aptroot, A.; Coppins, B.J.; Fletcher, A.; Gilbert, O.L.; James, P.W.; Wolseley, P.A. *The Lichens of Great Britain and Ireland*; British Lichen Society: London, UK, 2009; 1046p.
53. Ignatov, M.S.; Ignatova, E.A. *Moss Flora of the Middle European Russia. Sphagnaceae–Hedwigiaceae*; Scientific Publishing Association: Moscow, Russia, 2003; Volume 1, pp. 1–608.
54. Ignatov, M.S.; Ignatova, E.A. *Moss Flora of the Middle European Russia. Fontinalaceae–Amblystegiaceae*; Scientific Publishing Association: Moscow, Russia, 2004; Volume 2, pp. 609–960.
55. Hodgetts, N.G.; Söderström, L.; Blockeel, T.L.; Caspari, S.; Ignatov, M.S.; Konstantinova, N.A.; Lockhart, N.; Papp, B.; Schröck, C.; Sim-Sim, M.; et al. An annotated checklist of bryophytes of Europe, Macaronesia and Cyprus. *J. Bryol.* **2020**, *42*, 1–116. [[CrossRef](#)]
56. Frank-Kamenetskii, V.A. *X-ray Research of the Main Types of Rock-Forming Minerals (Layered and Framework Silicates)*; Leningrad: Nedra, India, 1983; p. 359. (In Russian)
57. *Determination of Macro- and Microelements (Including Rare Earths) by Inductively Coupled Plasma Mass Spectrometry*, Method No. 10; SPb: TsL VSEGEI. 2010; 5. (In Russian)
58. Samecka-Cymerman, A.; Kempers, A.J. Differences in concentration of heavy metals between native and transplanted *Pohlia nutans* (Hedw.) Lindb.—A case study from a dump exposed to industrial emissions in Poland. *Pol. J. Environ. Stud.* **2007**, *16*, 51–258.

59. Novinyuk, L.V.; Velinzon, P.Z.; Kulev, D.C. Sorption properties of chitin- and chitosan-glucan bio- complexes isolated from *Aspergillus niger* fungal mycelia biomass. *Appl. Chem. Biotechnol.* **2017**, *7*, 64–71. [[CrossRef](#)]
60. Gadd, G.M. Fungi and Yeasts for Metal Binding. In *Microbial Mineral Recovery*; Ehrlich, H., Brierley, C.L., Eds.; McGraw-Hill: New York, NY, USA, 1990; pp. 249–275.
61. Gutarowska, B.; Czyżowska, A. The ability of filamentous fungi to produce acids on indoor building materials. *Ann. Microbiol.* **2009**, *59*, 807–813. [[CrossRef](#)]
62. Sazanova, K.; Osmolovskaya, N.; Schiparev, S.; Yakkonen, K.; Kuchaeva, L.; Vlasov, D. Organic Acids Induce Tolerance to Zinc- and Copper-Exposed Fungi Under Various Growth Conditions. *Curr. Microbiol.* **2015**, *70*, 520–527. [[CrossRef](#)] [[PubMed](#)]
63. Stanković, J.D.; Sabovljević, A.D.; Sabovljević, M. Bryophytes and heavy metals: A review. *Acta Bot. Croat.* **2018**, *77*, 109–118. [[CrossRef](#)]
64. Kłos, A.; Czora, M.; Rajfur, M.; Waclawek, M. Mechanisms for Translocation of Heavy Metals from Soil to Epigeal Mosses. *Water Air Soil Pollut.* **2011**, *223*, 1829–1836. [[CrossRef](#)] [[PubMed](#)]
65. Shahid, M.; Ferrand, E.; Schreck, E.; Dumat, C. Behavior and Impact of Zirconium in the Soil-Plant System: Plant Uptake and Phytotoxicity. In *Reviews of Environmental Contamination and Toxicology*; Springer: Berlin/Heidelberg, Germany, 2013; Volume 221, pp. 107–127. [[CrossRef](#)]